Granular Matter (2021) 23:3
https://doi.org/10.1007/s10035-020-01065-3

BRIEF COMMUNICATION

Extending the Boussinesq model for impacts in granular media

Francisco Martínez[1] · **María P. Urrea**[1] · **Claudia M. Gonzalez**[1] · **Germán Varas**[2]

Received: 27 April 2020 / Accepted: 1 October 2020

Abstract
Granular impact phenomena have implications in many areas. A fundamental problem deals with the mechanical response of a granular medium under external loads, such as those derived from the impact of a rigid object on the top of the medium. Here, the load changes its magnitude and intensity during the impact, being also applied in much shorter intervals than those of a static load, where the Boussinesq model is usually valid. This dynamic has been poorly addressed in the literature, a void to which this study aims to contribute, where we measure the pressure distribution transmitted at the bottom of a uniform, dry granular layer under the action of gravitational impacts of a steel sphere of fixed diameter. Exploring different bed thicknesses and drop heights, it is found that the structure of this distribution follows a similar form to the Boussinesq model, which was proposed initially for static conditions. This surprising result opens up several questions and future research challenges that could help validate or refute this model in other scenarios.

Keywords Granular impact · Mechanical response · Pressure distribution

1 Introduction

Impact phenomenon has acquired a great interest in the last decades, due to its implications in different disciplines. In the field of geology, the study of this topic has allowed to extract information about Earth's data [1]. In soil mechanics, impacts are typically involved in compaction processes performed for the improvement of soil quality, its stability, and bearing capacity [2]. From the physical point of view, the study of impacts has allowed getting insight about properties of frictional resistance of granular media, their rheological behavior, and the mechanical response issue from the application of external loads. However, very few studies have addressed this topic. Boussinesq's model was a pioneer attempt to propose a general law describing the mechanical response in an inner point (r, z) (Fig. 1b) of a semi-infinite, homogeneous, linear and isotropic elastic medium under a single point-force in a static case,

$$P(r,z) = \frac{3F}{2\pi}\frac{1}{z^2}\left[\left(\frac{r}{z}\right)^2 + 1\right]^{-5/2} = \frac{F}{z^2}I_B(r,z), \tag{1}$$

where F is a point-force applied at the top, and I_B is the Boussinesq stress coefficient dependent on the coordinates of the stress point [3, 4]. Different experimental and numerical researches have measured the pressure distribution $P(r, z)$ at the bottom of granular piles under the action of a localized static forces [5–13]. In these cases, the physical characteristics of the material is far from Boussinesq's hypothesis, however the granular piles response is well represented by such distribution, as shown in 3D granular piles [5, 8], from the numerical solution of diffusion models of force chains in the assemblies of disks [6, 7] and a granular medium with large thicknesses [9, 10]. On the other side, it was also shown that introducing friction between the grains is possible to extend the validity of a Boussinesq model for stronger forces, reducing the effects of mechanical anisotropy of the

✉ Francisco Martínez
francisco.martinez@pucv.cl

María P. Urrea
maria.urrea.d@mail.pucv.cl

Claudia M. Gonzalez
claudia.gonzalez.b@pucv.cl

Germán Varas
german.varas@pucv.cl
https://fis.ucv.cl/gvaras/

[1] Escuela de Ingeniería Civil, Pontificia Universidad Católica de Valparaíso (PUCV), Av. Brasil 2147, Valparaiso, Valparaiso, Chile

[2] Instituto de Física, Pontificia Universidad Católica de Valparaíso (PUCV), Avenida Universidad 330, Valparaiso, Chile

Published online: 20 November 2020

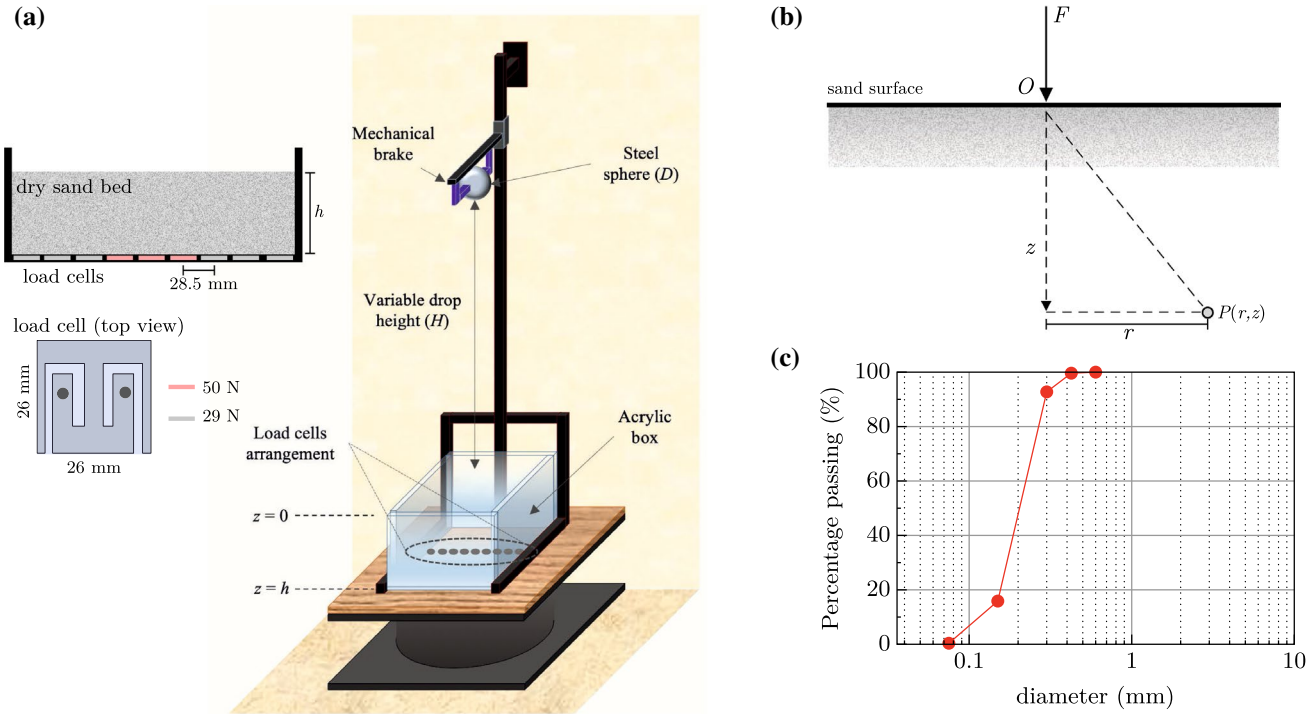

Fig. 1 **a** General view of the experimental set-up. A sandy-bed (height h) is deposited in an acrylic tank. A steel sphere (diameter D) is dropped from a height H. The impact is recorder throughout a series of load cells positioned at the bottom of the tank. The load cells are separated by a distance of 28.5 mm from center to center. The three central cells have a capacity of 50 N, while the lateral cells are 29 N. **b** Diagram of a point load at the surface. **c** Grain size distribution

pile [10, 11]. These results have given new insight into the general mechanical response in granular piles, but all of them deal with the scenario of single point-forces acting in static conditions.

In dynamic conditions the applied force happens in very short times, giving less time to grains to arrange during the impact and so affecting the topology of force networks [14, 15]. Very few studies have dealt with this case, for example, [16] measured both the deformation and stress field resulting from the impact of a horizontal bar in a 2D granular pile. This field shows a similar structure than those arising from uniform static planar loads [3, 4], suggesting that a pseudo-static approach could be reasonable to describe the mechanical response for an impact. To this concern, [17] conducted experiments on triggering mechanisms of avalanches measuring the force at the bottom of a wet sandy bed, showing that the peak of the acceleration-signal could be used to describe the dynamics after the impact. Finally, [18] performed DEM simulations of the impact of spheres on 3D granular piles, measuring the local compaction and relative density of the soil under the dynamical load getting insight about the effectiveness of this phenomena for soil compaction. The aim of the present experimental study is to show, for the first time, the response of a uniform and dry granular bed under the action of a load induced by the impact of a spherical intruder on the top of the bed, measuring the bottom pressure distribution generated by such impact.

2 Experimental setup

According to the *Unified Soil Classification System*, the material used corresponded to poorly graded sand (SP). Its size distribution is shown in Fig. 1c and its properties are summarized in Table 1. We deposited a natural clean and dry sandy bed in an acrylic (Young's modulus $E = 3.10$ Gpa) deposit of square section ($L \times L$) of 265 mm $\times$ 265 mm, with 10 mm of bottom-thickness, 5 mm wall-thickness and a variable height in the range $h = 90 - 190$ mm, as shown in Fig. 1a. The intruder is a steel sphere with diameter $D = 60$ mm and density $\rho = 7.9$ g/cm^3. In the experiments, the sphere was dropped from different heights ($H = 0.50, 0.75$ and 1.00 m), measured from the center of the sphere to the surface of the material. The dropping system consists of a mechanical brake deactivated manually and smoothly so that the intruder is released with zero initial speed. Some studies have shown the sensitivity and asymmetry of the results when varying the inclination of the force applied at the top [12]. To prevent these effects, we use an Automatic

Table 1 Sand properties—extracted from the dunes of Concon, Valparaiso region

Property	Value	Units
Solid density (ASTM D854)—G_s	2.770	–
Particle diameter—D_{10}	0.115	mm
Particle diameter—D_{30}	0.170	mm
Particle diameter—D_{60}	0.223	mm
Coefficient of uniformity—C_u	1.194	–
Coefficient of curvature—C_c	1.113	–
Soil classification	SP	–

*D_{10}, D_{30} and D_{60} corresponds to the diameters of the particles for which 10%, 30% and 60% of the particles are finer than those sizes respectively

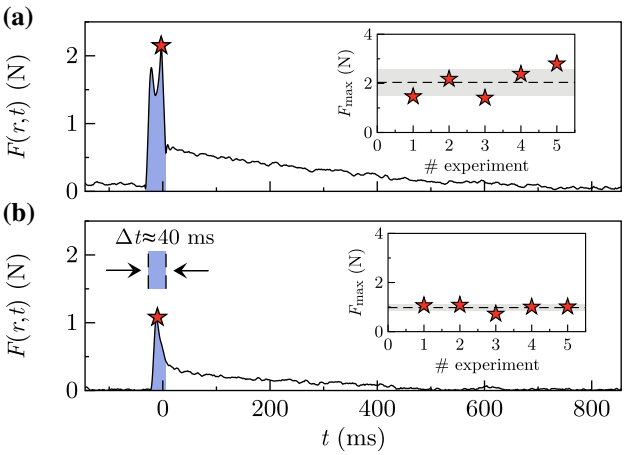

Fig. 2 Force time series of the impact at **a** $r = 0$ mm (center) and **b** $r = 114$ mm (at the side) for a falling height $H = 1$ m and grains height $h = 190$ mm. We set $t = 0$ ms at the instant where the load is maximum ($F_{\max}$). The colored area corresponds to the duration of the impact $\Delta t \approx 40$ ms. (inset) Peak values obtained for each repetitions. The dashed line corresponds to the average value $\langle F_{max} \rangle$ and the gray zone to the error bars given by the standard deviation. $\langle F_{\max} \rangle = 2.0 \pm 0.5$ N ($\delta = 25\%$) and $\langle F_{\max} \rangle = 0.98 \pm 0.13$ N ($\delta = 13\%$) for $r = 0$ mm and $r = 114$ mm respectively

Level Surveying Instrument (Spectra Precision AL32M) to assure the verticality of the dropping system and then, ensuring that the impact point always occurs at the center of the granular surface. A metallic, rigid structure supports the acrylic deposit and the dropping system. Additionally, it permits to change the drop height of the intruder. The granular over-pressure induced by the impact at the position (r, z) into the medium is denoted by $P(r, z)$, where r range from $r = [-114, 114]$ mm and z is the granular depth (positive downwards) where $z = 0$ denotes the position of the surface (see Fig. 1a). A collection of nine loading-cells (model TAL 106, HT sensor Technology Co.) are disposed at the bottom of the container. All of them equally distributed along the central axis of the tank and covered by a skinny polyethylene layer (10 µm thickness) in order to prevent direct contact with the grains that may cause the sensor to malfunction or break. The cells has a surface contact area $S = 26 \times 26$ mm^2 and 1 mm off thickness, whose nominal loading capacity ranges from 29 N (side load cells) up to 50 N (center load cells). Additionally, an electronic acquisition system records in a computer the force signals emitted simultaneously by each sensor at a sampling rate of 2.5 kS/s. Taking this into account, at the bottom of the tank ($z = h$) the average pressure is given by $P(r, h) = F_{\max}/S$, where $F_{\max}$ is the peak value of time-force series of the sensor located at the position (r, h) and S is the contact area of each sensor.

Finally, the sandy beds were formed by pluviation technique. It was used the procedure proposed for González and Romo [19] that consists of combining sieves with a perforated plate to obtain reproducibly homogeneous sand deposits. For each test, this density was calculated by dividing the mass (M) of the grains by the volume (V) occupied by them in the acrylic box ($\rho_s = M/V$). The mass of the particulate material was measured before running every experiment, under dry conditions. For this research, the pluviation procedure permits obtain a relative density $\rho_s = [1.43 - 1.54]$ g/cm^3 with a mean value of $\bar{\rho}_s = 1.47$ g/cm^3. Taking these elements into account and considering that the recipient is not deeper enough to observe a Janssen-like effect, the theoretical (hydrostatic) granular pressure prior to the impact can be roughly approximated by $\rho_s g h$. This pressure falls in the range 1.46–3.08 kPa, much lower than the nominal capacity of the sensors.

3 Force series

Each sensor records a force time signal denoted by $F(r, t)$ where r indicates the horizontal position. Figure 2a shows a typical result of this signal due to the impact of a sphere falling from a height of $H = 1.00$ m and bed thickness $h = 190$ mm. We recall that the loading-cells measure only the excess of force due to the impact and not the static pressure generated by the weight of the granular column. At first, we observe that in all the series the typical impact duration is of the order of $\Delta t \approx 40$ ms. During the phenomena, the force signal generally shows an explosive increase right after the impact in a time interval of 20 ms reaching a peak value $F_{\max}$. Then, the force quickly drops to smaller, but non-strictly zero values, following a relaxation curve which arises from the mechanical behavior of the load cell. This decreasing behavior typically occurs in a time of order 20 ms, depending on the experimental conditions and the position of the cell. The total duration of the interval is of the order than the typical stopping time reported for impact phenomena in sandy beds (e.g. [20–22]). We define the time origin ($t = 0$) at the instant where the load is maximum ($F_{\max}$).

Figure 2b shows that the farther point ($r = 114$ mm) has a clear decrease in the force and more reproducible results. This is left in evidence comparing the peaks values issued from five experiments performed under the same initial conditions (inset Fig. 2). At $r = 0$ we observe a higher dispersion of data, above than the sensors located far from the center.

4 Granular pressure distribution

Figure 3a show the bottom pressure measured at different bed thickness. As expected, for a given position r, $P(r, h)$ reduces at increasing h. For each bed thickness, the pressure tends to decrease as it moves away from the point of impact. At the same time, the pressure distribution reduces

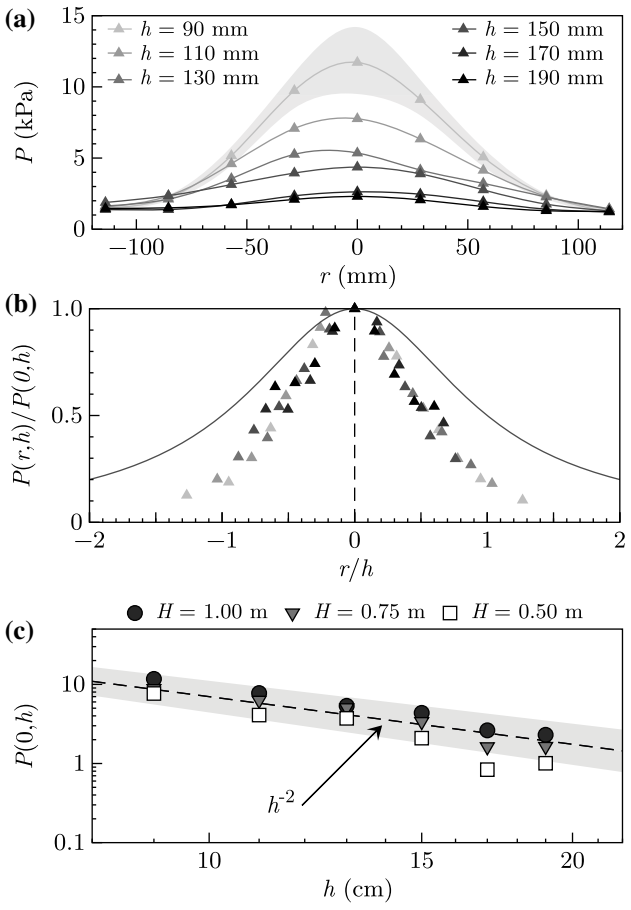

Fig. 3 **a** Pressure distribution $P(r, h)$ for $H = 1.0$ m and different bed thickness h, as a function of the horizontal distance r. The continuous lines are a guide to the eye and the gray area indicates the error. **b** Normalized distributions $P(r, h)/P(0, h)$ versus r/h for the same experimental data. The continuous line is a Lorentzian profile. **c** Distribution of central pressure points $P(0, h)$ compared to bed thickness h for falling heights $H = 0.5, 0.75, 1.0$ m. The segmented line correspond to power law $P \propto h^{-m}$ with $m = 2$. The shaded zone correspond to a variation of the exponent $m = 2.0 \pm 0.2$

for decreasing impact energies suggesting the existence of a critical bed thickness where the cells are not significantly sensitive to the impact. According to our data, this thickness falls systematically in the range $h \geq 190$ mm.

In order to get a quantitative insight about the structure of $P(r, h)$ we compare the normalized distribution $P(r, h)/P(0, h)$ with r/h for all the experiments (Fig. 3b). The data seems to collapse in a reasonable single distribution suggesting an scaling relation of the type $P(r, h) \propto P(0, h) f(r, h)$, where f is a fitting function to be determined from the experimental points and $P(0, h)$ is the bottom pressure just below surface's impact point. These normalized pressure distributions are sharper than a typical Lorentzian profile, as remarked by [5, 6]. Figure 3c shows the distribution of $P(0, h)$ as a function of h, with H as a parameter. We observe a tendency in $P(0, h)$ to increase with H for a given bed thickness. However, this variation in H is weak allowing these points to be closely described by the scaling law $P(0, h) \propto h^m$, where $m \approx -2$ is the fitting slope. This finding is in agreement with the structure given by Eq. (1), conducting to the scaling $P(r, h) \propto h^{-2} f(r, h)$. With all these elements, in the Fig. 4a we show the distribution of Ph^2 versus r/h obtained under different dropping heights. The dispersion of these curves become particularly significant for $H = 0.5$ m, but it decreases for increasing dropping heights. Taking this into account, we have drawn a single fitting mean curve for each distribution given for the function $f(r, h) \propto (1 + (r/h)^2)^{-5/2}$. These findings can be then summarized in the formula,

$$P(r, h) = \frac{K}{h^2}\left(1 + (r/h)^2\right)^{-5/2}, \tag{2}$$

where K is a fitting parameter taking the values 46.1 ± 2.3 N, 68.5 ± 2.3 N and 88.8 ± 2.0 N, for $H = 0.5, 0.75$ and 1 m respectively. Looking at the units of this parameter, K should contain some information about the point-force being applied at the top of the granular surface, a topic that we will extend in the next section.

5 A simple point force model

To get insight about the force applied on the top we build a simple model for the instant point-force applied on the top of the material. This model is given by the sum of the intruder's weight (Mg) and a dynamical component issue from the kinetical momentum exchange at the impact,

$$F_D = Mg + \frac{1}{2}\rho S_t u^2, \tag{3}$$

where M is the mass of the intruder, ρ its density, S_t the projected area involved in the momentum exchange, and u

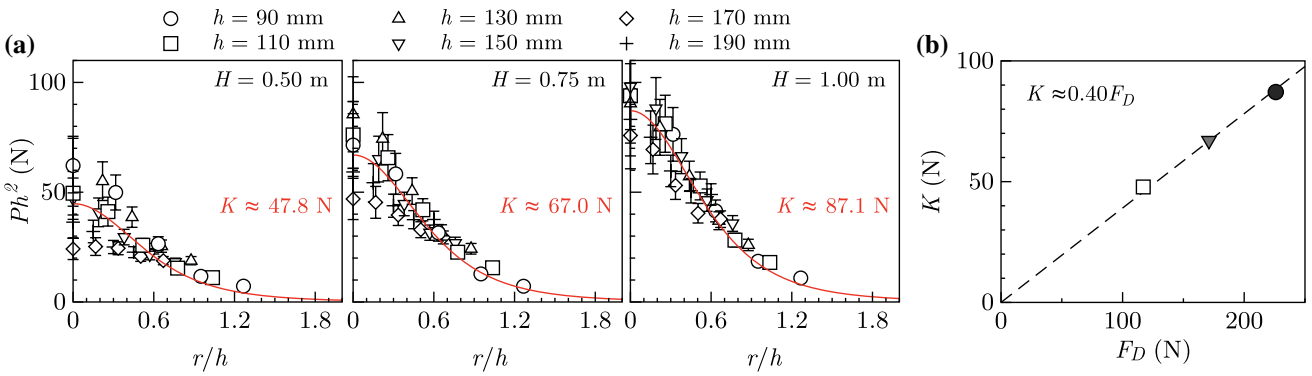

Fig. 4 **a** Force distribution Ph^2 for different drop heights H and bed thickness h. **a** (left) $H = 0.5$ m, (center) $H = 0.75$ m and (right) $H = 1.0$ m. The continuous lines correspond to the fit $K(1 + (r/h)^2)^{-5/2}$ where K depends on the dropping height. **b** Fitting parameter K vs the dynamics force F_D for (□) $H = 0.50$, (gray ▽) $H = 0.75$ m and (•) $H = 1.00$ m

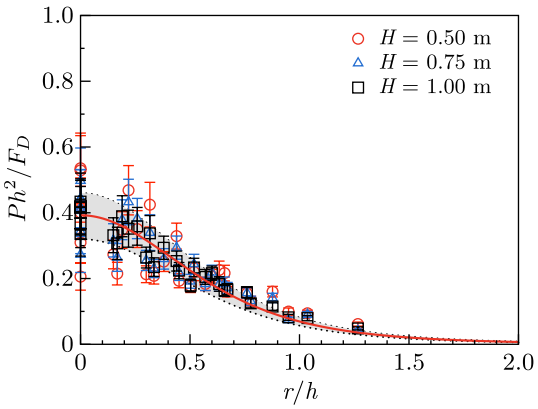

Fig. 5 Normalized bottom pressure distribution, for the three different falling heights. The continuous red line corresponds to the curve $\lambda(1 + (r/h)^2)^{-5/2}$ and the gray zone to an upper and lower bounds corresponding to 10% of variation of λ as a guide to the eye

the velocity of the sphere. By simplicity, we assume that $S_t = \pi R^2$ where R is the radius of the sphere and $u \simeq \sqrt{2gH}$ is the velocity right before the impact. The relation between K and F_D is shown in Fig. 4b. The results show a linear dependence between both quantities with a numerical constant $\lambda \approx 0.40$. As this factor include the terms of the dynamic, we propose that all the data can be normalized in the following way $P(r,h)h^2/F_D = \lambda(1 + (r/h)^2)^{-5/2}$. The right side of the last equation is a universal curve that depends only on the numerical factor λ. All the experimental results are summarized in Fig. 5. We observed a good agreement between the experimental data and the proposed model despite of the data dispersion. These results suggest a more general expression valid for a granular layer of thickness h in a low-velocity regime,

$$P(r,h) \simeq \frac{F_D}{h^2} I_B(r,h). \tag{4}$$

Finally, this simple expression extends the initial model proposed by Boussinesq for non-static conditions adding a dynamical component to the static point force.

6 Discussion and conclusion

In the present study, peak-pressure distributions at the bottom of a uniform, dry granular media with variable thickness, under the impact of a steel sphere in free fall are reported for the first time. These profiles looks similar to those reported in [5, 6]. Compared to the Boussinesq law (Eq. 1) we found that, even if our case is far from the hypothesis supporting the theoretical model (e.g., frictional grains, anisotropic media, quasi-uniform size distribution, dynamical surface force), the pressure distributions can be reasonably fitted by this formula. Despite the dispersion of the experimental data near the center (as shown in Fig. 2) the experimental results are well represented by a single curve of the type $P(r,h) \simeq F_D/h^m I_B(r,h)$, where F_D is a point-force model, and m is a fitting parameter close to 2, that in our range of parameters does not depend significantly on H. This point-force model considers both the contribution of intruder's weight and a dynamical term that takes into account the effect of H, through the momentum exchange between the intruder and the grains. To our knowledge, this result shows that in the range $H < 1$ m, it is possible to extend the original Boussinesq model for non-static conditions. This favorable result lets, however, some important open questions for future research. One of them is the need to study the granular response in experiments at high-level impact energy (*e.g.* when $H \gg 1$m), where granular stiffness could

strongly change and even induce fracture of the media. On the other hand, it is necessary to delve into the role played by the properties of the grains on this phenomenon, like particle shape, size-distribution, compacity and macroscopic inner friction and their relation with intruder's stopping time and the relaxation of the granular media. Some authors have found that this timescale is quasi-constant for high impact velocities, but it can increase significantly for lower impact speeds, suggesting that the grains rearrange differently depending on impact energy [21, 22]. Consequently, it is reasonable to think that the stopping time should have a relationship with the pressure peaks values measured at the bottom of the granular bed. We are aware of this fact and the possible uncertainties introduced on the determination of the peak-force, which certainly deserves further analysis in a future study. We will explore this and other possible mechanisms using the appropriate equipment for this type of measurements (*e.g.*, piezoelectric transducers). Finally, the geometry of the load is another topic to consider in this research, leading to other theoretical formulations different from the standard Boussinesq model. All of these considerations must influence the structure of the force network transmitted just under the impact point and, in consequence, the pressure distributions measured at the bottom of the granular pile.

Acknowledgements The authors acknowledge the Vicerrectoria de Investigación of the PUCV by the financial support of this research trough the project *Investigador Emergente* 039.371/19. We also thank Philippe Gondret and Aldo Tamburrino for their valuable comments and discussions on the article. Finally, we thank Hugo Tapia (PUCV) and Daniel Yunge (PUCV) for their technical support given during the construction of the experimental set-up.

Compliance with ethical standards

Conflict of interest The authors declare that they have no conflict of interest.

References

1. Melosh, H.J.: Impact Cratering. A Geologic Process. Oxford University Press, Oxford (1989)
2. Poran, C.J., Rodriguez, J.A.: Design of dynamic compaction. Can. Geotech. J. **29**(5), 796 (1992)
3. Murthy, V.N.S.: Geotechnical Engineering: Principles and Practices of Soil Mechanics and Foundation Engineering. CRC Press, Boca Raton (2008)
4. Bowles, J.E.: Foundation Analysis and Design. McGraw-Hill International, New York (1996)
5. Reydellet, G., Clément, E.: Green's function probe of a static granular piling. Phys. Rev. Lett. **86**, 3308 (2001)
6. Bouchaud, J.P., Cates, M., Claudin, P.: Stress distribution in granular media and nonlinear wave equation. J. Phys. I **5**(6), 639–656 (1995)
7. Bouchaud, J.P., Claudin, P., Levine, D., Otto, M.: Force chain splitting in granular materials: a mechanism for large-scale pseudo-elastic behaviour. Eur. Phys. J. E **4**(4), 451 (2001)
8. Bouchaud, J.P., Claudin, P., Clément, E., Otto, M., Reydellet, G.: The stress response function in granular materials. C. R. Phys. **3**(2), 141 (2002)
9. Goldenberg, C., Goldhirsch, I.: Force chains, microelasticity, and macroelasticity. Phys. Rev. Lett. **89**, 084302 (2002)
10. Goldenberg, C., Goldhirsch, I.: Friction enhances elasticity in granular solids. Nature **435**(7039), 188 (2005)
11. Goldenberg, C., Goldhirsch, I.: Effects of friction and disorder on the quasistatic response of granular solids to a localized force. Phys. Rev. E **77**, 041303 (2008)
12. Atman, A.P.F., Brunet, P., Geng, J., Reydellet, G., Combe, G., Claudin, P., Behringer, R.P., Clément, E.: Sensitivity of the stress response function to packing preparation. J. Phys. Condens. Matter **17**(24), S2391 (2005)
13. Atman, A.P.F., Brunet, P., Geng, J., Reydellet, G., Claudin, P., Behringer, R.P., Clément, E.: From the stress response function (back) to the sand pile "dip". Eur. Phys. J. E **17**(1), 93 (2005)
14. Clark, A.H., Kondic, L., Behringer, R.P.: Particle scale dynamics in granular impact. Phys. Rev. Lett. **109**, 238302 (2012)
15. Clark, A.H., Petersen, A.J., Kondic, L., Behringer, R.P.: Nonlinear force propagation during granular impact. Phys. Rev. Lett. **114**, 144502 (2015)
16. Nazhat, Y., Airey, D.: The kinematics of granular soils subjected to rapid impact loading. Granular Matter **17**(1), 1 (2015)
17. Takizawa, S., Niiya, H., Tanabe, T., Nishimori, H., Katsuragi, H.: Impact-induced collapse of an inclined wet granular layer. Physica D Nonlinear Phenom. **386–387**, 8–13 (2019)
18. Ma, Z., Liao, H., Ning, C., Liu, L.: Numerical study of the dynamic compaction via DEM. Jpn. Geotech. Soc. Spec. Publ. **1**, 17 (2015)
19. Gonzalez, C.M., Romo, M.P.: Nueva técnica de pluviación para formar depósitos de arena. Serie azul del Instituto de ingenieria. Universidad Nacional Autónoma de Mexico, SID 691 (2015)
20. Ji, S., Chen, X., Li, P., Yan, Y.: Granular matter: a special buffer for impact load. AIP Conf. Proc. **1542**(1), 401 (2013)
21. Katsuragi, H., Durian, D.J.: Unified force law for granular impact cratering. Nat. Phys. **3**(6), 420 (2007)
22. Seguin, A., Bertho, Y., Gondret, P., Crassous, J.: Sphere penetration by impact in a granular medium: a collisional process. EPL (Europhys. Lett.) **88**(4), 44002 (2009)